



Obrabotka metallov -

Metal Working and Material Science

Journal homepage: http://journals.nstu.ru/obrabotka_metallov






Structure of Inconel 625 alloy blanks obtained by electric arc surfacing and electron beam surfacing

Aleksandr Boltrushevich^{1, a}, Nikita Martyshev^{1, b, *}, Victor Kozlov^{1, c}, Yulia Kuznetsova^{2, d}

¹ National Research Tomsk Polytechnic University, 30 Lenin Avenue, Tomsk, 634050, Russian Federation

² Admiral Ushakov State Maritime University, 93, Lenin Ave., Novorossiysk, 353924, Russian Federation

^a  <https://orcid.org/0000-0001-9971-7850>,  aeb20@tpu.ru; ^b  <https://orcid.org/0000-0003-0620-9561>,  martjushev@tpu.ru;

^c  <https://orcid.org/0000-0001-9351-5713>,  kozlov-viktor@bk.ru; ^d  <https://orcid.org/0000-0002-1388-6125>,  julx@bk.ru

ARTICLE INFO

Article history:

Received: 13 September 2024

Revised: 05 October 2024

Accepted: 10 October 2024

Available online: 15 December 2024

Keywords:

Additive manufacturing

Inconel 625

Electric arc surfacing

Electron beam surfacing

Microstructure

Funding

This research was supported by TPU development program.

Acknowledgements

The research was carried out at the equipment of the Engineering Center “Design and Production of High-Tech Equipment” and the shared research facility “Structure, mechanical and physical properties of materials”.

ABSTRACT

Introduction. Development of the manufacturing industry has led to the emergence of new methods for manufacturing blanks and parts. One of these new promising methods is additive manufacturing and, in particular, electric arc and electron beam surfacing technologies. The use of these technologies in the production of blanks from heat-resistant materials provides a number of significant advantages. The paper presents the results of a study of the microstructure of *Inconel 625* specimens obtained using *EBAM* and *WAAM* technologies. **The purpose of the work** is a comparative analysis of the microstructure of *Inconel 625* nickel alloy blanks obtained using *EBAM* and *WAAM* technologies. **Methods and materials.** The paper examined specimens obtained using *EBAM* and *WAAM* technologies. The specimens were manufactured using equipment developed at Tomsk Polytechnic University. Metallographic studies, scanning electron microscopy were carried out, and the microhardness of the obtained specimens was determined. **Results and discussion.** Comparison of specimens obtained by two different additive printing technologies *EBAM* and *WAAM* showed general patterns of structure formation that appear when using additive technologies. The specimens have a dendritic microstructure and contain zones rich in *Ti*, *Mo* and *Nb*, which is typical for nonequilibrium cooling. Pores are also observed in the specimens. The grains in the specimens have a predominantly elongated shape and are oriented in the direction of heat removal. The length of the grains reaches 1 mm. Differences in the specimens are observed in the number of formed inclusions of intermetallic compounds, in the number of formed pores, in the size of the grains. The *EBAM* technology provides more uniform structure. The difference in hardness between *EBAM* and *WAAM* is about 3.5 %. At the same time, the speed of specimen production using the *WAAM* technology is significantly higher.

For citation: Boltrushevich A.E., Martyshev N.V., Kozlov V.N., Kuznetsova Yu.S. Structure of Inconel 625 alloy blanks obtained by electric arc surfacing and electron beam surfacing. *Obrabotka metallov (tekhnologiya, oborudovanie, instrumenty) = Metal Working and Material Science*, 2024, vol. 26, no. 4, pp. 206–217. DOI: 10.17212/1994-6309-2024-26.4-206-217. (In Russian).

Introduction

In recent years, additive manufacturing has been rapidly expanding its scope of application due to its unique advantages. This manufacturing method allows the creation of complex-shaped parts with high precision, using a variety of materials, from plastic to metal, while significantly reducing time and costs compared to traditional technologies [1–4]. Depending on the requirements for the final product, specialists

* Corresponding author

Martyshev Nikita V., Ph.D. (Engineering), Associate Professor
National Research Tomsk Polytechnic University,
30 Lenin Avenue,
634050, Tomsk, Russian Federation
Tel.: +7 3822 60-62-85, e-mail: martjushev@tpu.ru

apply different technologies of additive manufacturing. Active development of additive technologies (*AT*) leads to a reduction in the cost of products manufactured with its help. This allows for the rapid production of parts and blanks of not only complex shapes, but also simpler shapes from expensive materials [5, 6]. An example of such parts can be flanges made of heat-resistant materials. When using *AT*, there is no need to make a hole and the volume of material removed due to subtractive machining is also reduced. This makes the use of *AT* in this case economically justified. Also, the use of *AT* for the production of flanges allows it to be manufactured to a specific size, which provides even greater savings in time and costs compared to the production of a similar part from rolled steel [7–9].

Electron beam (*EBAM*) and arc printing (*WAAM*) are the most suitable technologies for the rapid production of simple flange-type parts made of heat-resistant materials and, in particular, *Inconel* [10].

EBAM uses a high-power electron beam to melt a metal wire material, which is surfaced layer by layer to form the desired part. This method can create large size parts with high density and strength [11–14]. One of the key advantages of additive manufacturing is its ability to create complex 3D components with greater speed and flexibility compared to traditional methods such as milling or casting [15, 16]. 3D printing can reduce the number of manufacturing steps, minimize material waste, and create parts that cannot be made by other methods. This opens up new opportunities for engineers, allowing them to bring their boldest ideas to life [17–20].

Vacuum surfacing of blanks using *EBAM* technology makes it possible to significantly accelerate the workpiece fabrication process in comparison with *SLS* (*selective laser sintering*) technology. However, this is a rather expensive and labor-intensive method of parts manufacturing [21, 22]. A greater reduction in cost and simplification of the workpiece fabrication technology can be achieved using *WAAM* technology. This technology uses arc welding to surface metal wires layer by layer to form three-dimensional objects. *WAAM* makes it possible to create large-sized parts much faster than other additive technologies such as electron beam surfacing. *WAAM* is suitable for producing parts from a variety of metals including steel, titanium and nickel alloys [23–25]. The disadvantages of this technology are the possibility of porosity formation due to printing in a gas environment, as well as worse quality of the printed surface.

The features of *EBAM* and *WAAM* technologies will affect the structure and properties of the resulting blanks. The *EBAM* technology is currently used quite rarely for printing heat-resistant alloys [26, 27]. This is due to the relatively low prevalence and novelty of this technology. Printing heat-resistant alloys with the help of *WAAM* technology is also not often used. Printing of heat-resistant alloys by this technology has a number of technological difficulties. For these reasons, there are very few works devoted to the printing of heat-resistant nickel alloys by *EBAM* and *WAAM* technologies [28–31].

The purpose of this work is to conduct a comparative analysis of microstructure of workpieces from nickel alloy *Inconel 625* obtained by *EBAM* and *WAAM* technologies.

Methods and materials

A common nickel alloy of *Inconel 625* was chosen as a material for specimen fabrication. The specimens were printed with a 1.2 mm diameter wire. Printing was carried out on a substrate made of stainless steel with dimensions of 110×110×20 mm. The substrate was placed over the back plate and clamped tightly. The back plate was used to apply molten raw material to the part. It acts as a protection against melt penetration into the substrate and damage to the table.

In the printing unit used for printing, it was possible to adjust the position of the wire feeder. The position was adjusted in relation to the electron beam and the workpiece to be printed. This ensured the stability of the material transfer. During the welding process, a bridge of molten metal was created between the fuse and the molten bath [32, 33].

The chemical composition of wire material used for electron beam printing is shown in Table 1.

Printing of the first group of specimens was carried out on an electron beam wire surfacing unit manufactured at Tomsk Polytechnic University. The printing of the second group of specimens was carried out on an electric arc wire surfacing unit, also manufactured at Tomsk Polytechnic University.

Chemical composition of *Inconel 625* nickel alloy wire

Chemical element	<i>Ta</i>	<i>Al</i>	<i>Nb</i>	<i>Mo</i>	<i>Cr</i>	<i>Si</i>	<i>Fe</i>	<i>Co</i>	<i>Ti</i>	<i>Mn</i>	<i>Ni</i>
%	0.3	0.38	2.8	7.5	22.5	0.8	1.3	0.2	0.35	0.1	63.68

Four types of specimens were printed during the experimental work. Vertically and horizontally orientated specimens of each of the investigated technologies (*EBAM* and *WAAM*) were made.

Cross sections of the specimens were made to investigate the microstructure. The microstructure was revealed using an etchant consisting of a mixture of concentrated nitric HNO_3 (67 wt. %) and hydrochloric HCl (33 wt. %) acids taken in a ratio of 1:3 by volume. Microstructural studies were carried out using a metallographic microscope *MMP-1* manufactured by *BIOMED*. Photographs of the microstructure were obtained using a *DCM-510 SCOPE* video eyepiece. Microhardness was measured using an automatic complex based on the *EMCO-TEST DuraScan-10* microhardness tester. The measurements were carried out on the same specimens on which metallographic studies were carried out. Measurements were carried out with a *Vickers* indenter at a load of 1 kgf with a dwell time of 10 s.

Results and discussion

First of all, specimens were obtained for the research. Four specimens were obtained, two specimens using each of the *EBAM* and *WAAM* technologies. Specimens of vertical orientation (Figure 1 *a*, *c*) and horizontal orientation (Figure 1 *b*, *d*) were obtained. From the above pictures, it can be seen that the accuracy and surface quality of the specimens obtained by *EBAM* is higher. There is less metal spatter than when surfacing using an arc. Also, the cooling rate of specimens obtained by *EBAM* is lower than with *WAAM* printing. With *EBAM*, heat dissipation is difficult due to the lack of atmosphere. In *WAAM* surfacing of *Inconel*, helium is used. In addition, it is evident that the *EBAM* specimen has a greater number of layers. In *WAAM* surfacing, the thickness of printed layer is greater and the printing speed is higher. But this is accompanied by significant temperature fluctuations. The stresses caused by these temperature fluctuations cause deformation of the substrate, even when it is about 5 mm thick. In this case, vertical orientation of the specimens gives a higher speed, but at the same time higher stresses arise. With horizontal orientation, the specimen cools down more uniformly. This is reflected in a less deformation of the substrate.

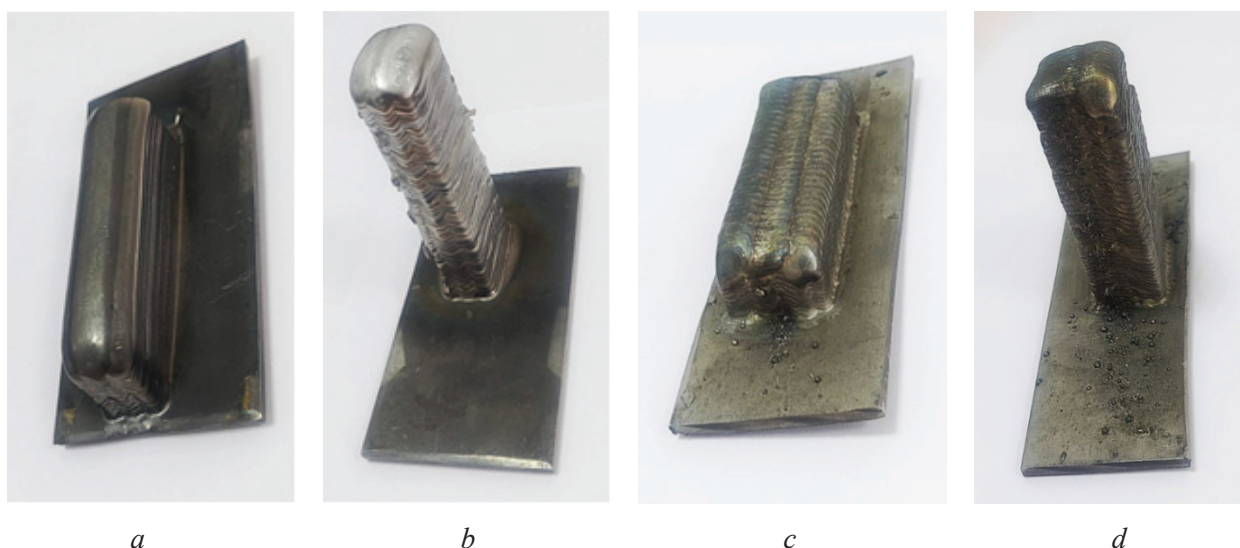


Fig. 1. Photos of specimens obtained using various additive technologies:

a – horizontal specimen obtained using *EBAM* technology; *b* – vertical specimen obtained using *EBAM* technology;
c – horizontal specimen obtained using *WAAM* technology; *d* – vertical specimen obtained using *WAAM* technology

The microstructure of *Inconel* 625 specimens obtained using *EBAM* and *WAAM* technologies is shown in Figure 2, *a–d*. This figure shows micrographs taken with an optical microscope in the center of the specimen. An elongated cellular structure with brightly colored particles in the interdendritic regions can be seen. The presence of dendritic structure is also clearly visible in all specimens. For horizontal specimens for both technologies, the dendrites have long first-order axes, while the second-order axes are practically absent. For vertical specimens, the cooling rate is lower and second-order axes have time to form; the embryos of third-order axes can be seen in some places. The difference in dendrite development is clearly visible for *EBAM* technology (Fig. 2, *a* and Fig. 2, *b*). In addition, it is evident from the shown microstructure, that the grains are textured. The texture is more developed for vertical specimens due to the higher cooling rate.

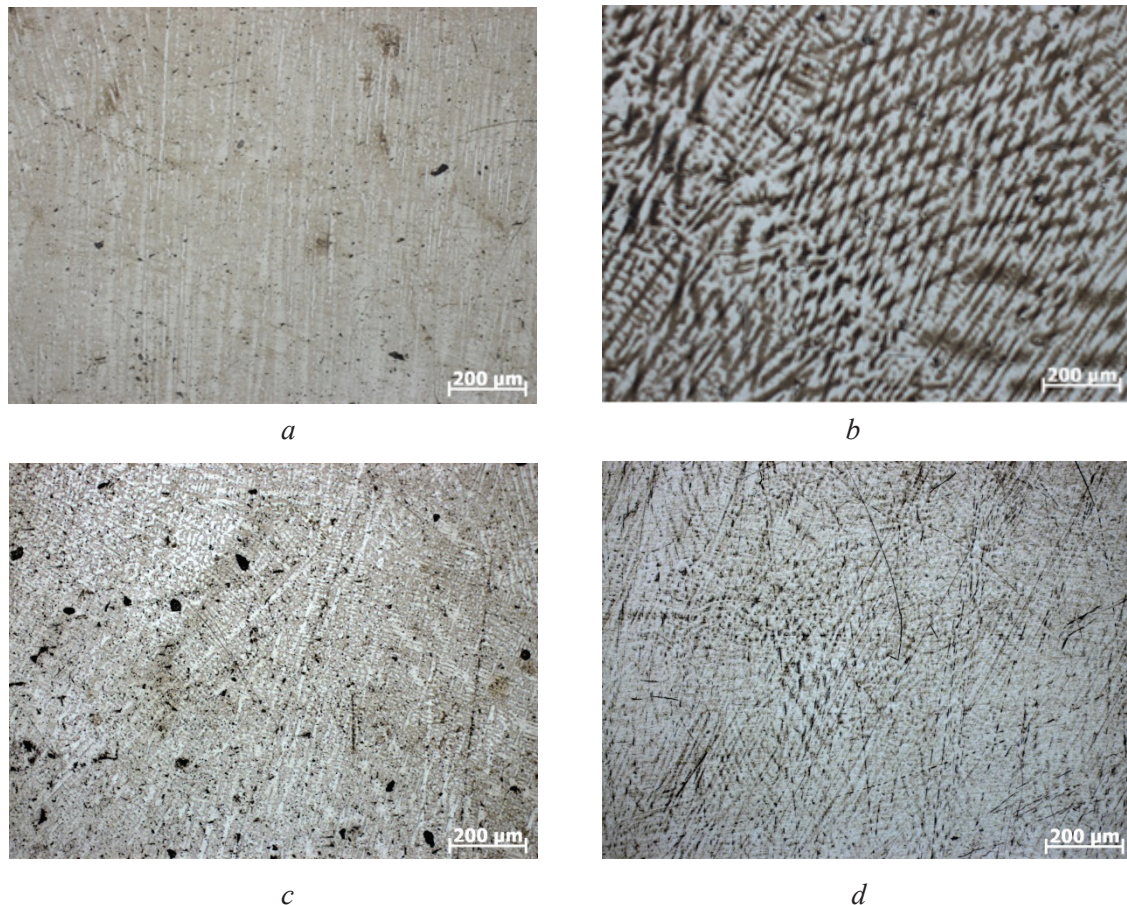


Fig. 2. Microstructure of specimens obtained using various additive technologies:

a – horizontal specimen obtained using *EBAM* technology; *b* – vertical specimen obtained using *EBAM* technology; *c* – horizontal specimen obtained using *WAAM* technology; *d* – vertical specimen obtained using *WAAM* technology

Certainly, different cooling rates lead to the formation of different grain sizes in the specimens. At the same time, in general, the same tendency is observed for all technologies under study. The grains have a dendritic structure; the grains are elongated in the direction of heat removal. The length of grains increases with distance from the substrate. For vertical specimens the cooling rate is lower and the grain length on the obtained specimens can reach 0.8–0.9 mm (vertical *EBAM* specimens). For horizontal specimens, the grain length reaches 0.3–0.5 mm. These data are in agreement with the results of other researchers. In [6], a specimen of *Inconel* 625 fabricated using the *SLM* technology had a grain length of about 1 mm. Specimens of *Inconel* 718 produced using the direct laser additive fusion process in the work [32] had a grain length of 3 mm. The authors of [11, 16], showed that the equiaxed grains are mainly located at the bottom, close to the *Inconel* 625 substrate. When moving away from the substrate, the grains elongate, texture appears and the length of the grains increases significantly. Our results are in good agreement with the data of these authors.

The regularities of the structure formation of specimens when printing with *EBAM* and *WAAM* technologies are similar to *SLM* technology. The difference is observed mainly in the sizes of phase components.

The scanning electron microscopy (*SEM*) photographs of the surface of the printed *Inconel 625* specimens are shown in Figure 3. As in other studies [2, 4, 5, 7], fine micron-sized particles were often observed in the surfaced material. Considering the particle size of the phase constituents, its quantitative chemical analysis can be difficult due to the *XRD* signal emanating from the matrix material. The chemical composition of the fabricated material (Table 2) is largely similar to that of the wire used for surfacing, except for elements such as iron and aluminum, the content of which was lower. The particles marked as **3** in Figure 3 showed more *Nb*, *Mo*, *Ti* and *C* (Table 2). This indicates the presence of *MC* carbides. A similar situation was also observed in *Inconel 625* alloy fabricated by additive manufacturing method by the authors of [2, 4, 7]. The phase marked as point **2** had elevated amounts of *Ni*, *Nb*, *Cr* and *Mo* without the presence of carbon (Table 2). This indicates the presence of intermetallic phases.

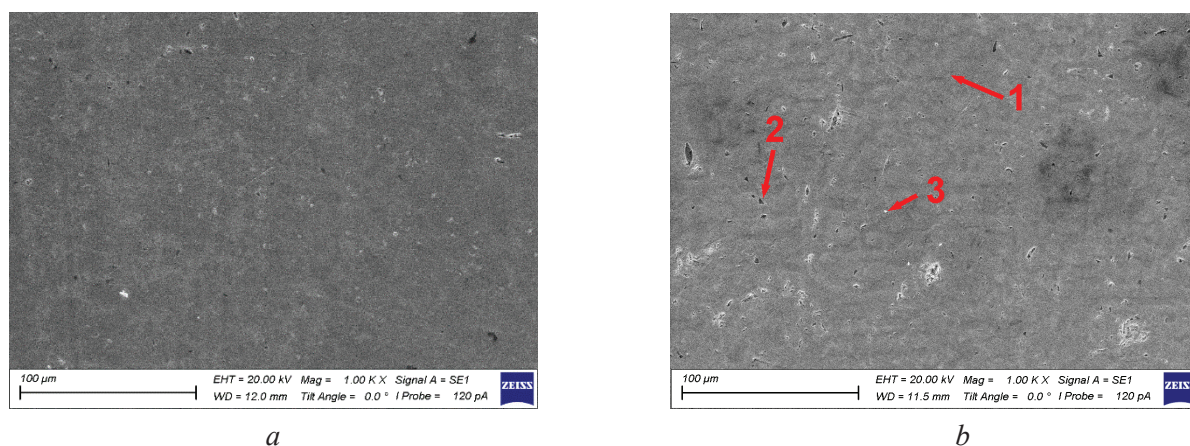


Fig. 3. SEM of specimens obtained using various additive technologies:

a – horizontal specimen obtained using *EBAM* technology; *b* – horizontal specimen obtained using *WAAM* technology

Table 2

Chemical composition of the manufactured material

Study area from Figure 3, %	<i>Ni</i>	<i>Cr</i>	<i>Nb</i>	<i>Mo</i>	<i>Si</i>	<i>Fe</i>	<i>Al</i>	<i>Ti</i>	<i>C</i>
1	64.0	22.3	1.1	4.2	0.7	1.3	0.1	0.1	6.2
2	2.7	3.5	7.2	0.5	–	0.7	–	48.1	37.3
3	38.5	21.6	16.7	8.9	4.1	0.7	0.2	0.2	9.1

The microhardness of the blanks was determined by the *Vickers* method at a load of 1 kgf with a dwell time of 10 s, as the average of twenty points at different locations (Figure 4).

The analysis of microhardness indices (Table 3) shows that the hardness of vertical specimens is lower than that of horizontal specimens. Both for specimens obtained by *EBAM* technology and for specimens obtained by *WAAM* technology, this discrepancy is about 3.5 %. It is also evident from the data obtained that the dispersion of hardness values for vertically orientated specimens is significantly higher than for horizontally orientated specimens. This can be explained by a smaller temperature gradient during the printing process. For horizontal specimens, heat dissipation is more intensive, which leads to the formation of more significant temperature gradients and the formation of a less homogeneous structure. This is consistent with the data of the microstructure analysis of the specimens. In vertically oriented specimens more homogeneous structure is formed; these specimens have fewer pores, fewer inclusions of intermetallic compounds in comparison with horizontally oriented specimens.

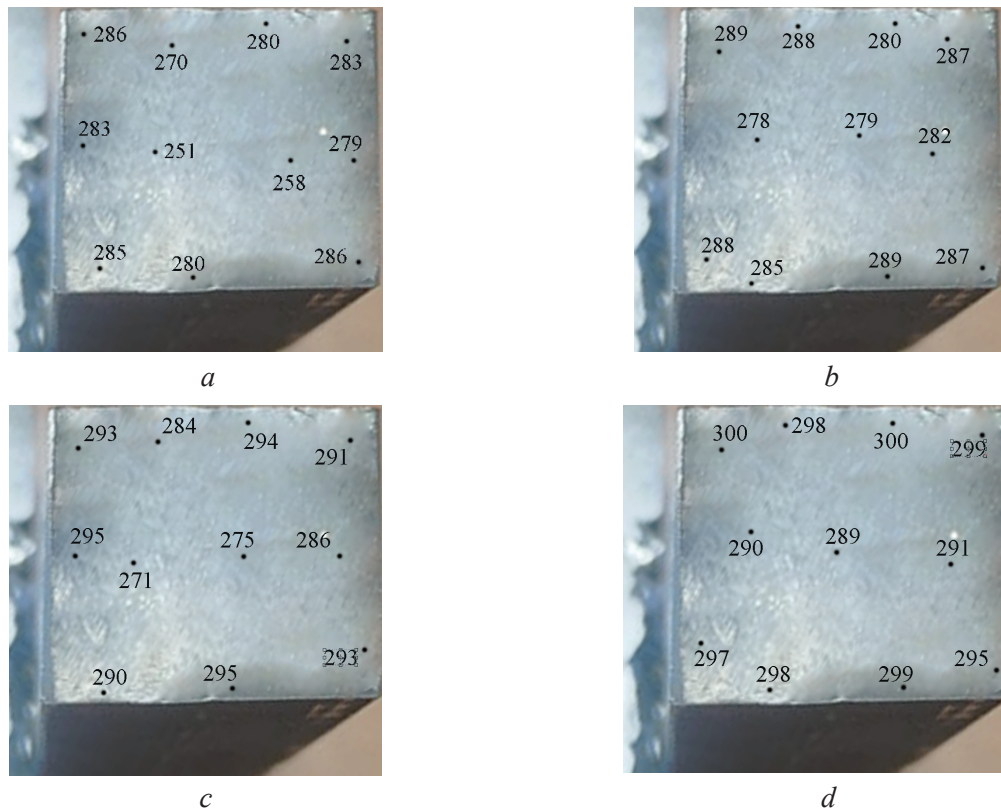


Fig. 4. Microhardness of specimens obtained using various additive technologies: *a* – horizontal specimen obtained using *EBAM* technology; *b* – vertical specimen obtained using *EBAM* technology; *c* – horizontal specimen obtained using *WAAM* technology; *d* – vertical specimen obtained using *WAAM* technology

Table 3

Microhardness of specimens

Specimen manufacturing technology	Specimen orientation	Maximum hardness, HV	Minimum hardness, HV	Average hardness, HV
<i>WAAM</i>	Horizontally	251	286	273.0
<i>WAAM</i>	Vertically	278	289	284.2
<i>EBAM</i>	Horizontally	271	295	283.4
<i>EBAM</i>	Vertically	289	300	294.4

The data also show that the hardness of the specimens obtained by *EBAM* technology is higher than that of the specimens obtained by *WAAM* technology. This is also in good agreement with the results of microstructure analysis. *EBAM* technology due to printing in vacuum gives a smoother cooling process of specimens. This leads to the formation of a more homogeneous structure with higher hardness.

Conclusions

The comparison of the specimens produced by two different additive printing technologies (*EBAM* and *WAAM*) was carried out taking into account the differences in the resulting microstructure and hardness. Printing using both technologies resulted in dendritic microstructure of the specimens. All specimens contained zones rich in *Ti*, *Mo* and *Nb*. Pores were also observed in the specimens. The grains in the specimens had a predominantly elongated shape and were oriented in the direction of heat removal. The length of the grains reached values of 1 mm. These features were observed for all the specimens obtained, regardless of the manufacturing technology or the orientation of the specimen during printing.

Differences in the specimens were observed in the number of intermetallic inclusions formed and in the grain size. Thus, the *EBAM* technology gives more homogeneous structure. As a result, the hardness of the specimens obtained by *EBAM* technology is higher than the hardness of the specimens obtained by *WAAM* technology at a similar orientation during printing. The difference in hardness between *EBAM* and *WAAM* is about 3.5 %. At the same time, the speed of production of specimens using *WAAM* technology is significantly higher.

References

1. Alvarez L.F., Garcia C., Lopez V. Continuous cooling transformations in martensitic stainless steels. *ISIJ International*, 1994, vol. 34 (6), pp. 516–521. DOI: 10.2355/isijinternational.34.516.
2. Li C., White R., Fang X., Weaver M., Guo Y. Microstructure evolution characteristics of Inconel 625 alloy from selective laser melting to heat treatment. *Materials Science and Engineering: A*, 2017, vol. 705, pp. 20–31.
3. Liverani E., Fortunato A. Additive manufacturing of AISI 420 stainless steel: process validation, defect analysis and mechanical characterization in different process and post-process conditions. *The International Journal of Advanced Manufacturing Technology*, 2021, vol. 117 (3–4), pp. 809–821. – DOI: 10.1007/s00170-021-07639-6.
4. Li S., Wei Q., Shi Y., Zhu Z., Zhang D. Microstructure characteristics of Inconel 625 superalloy manufactured by selective laser melting. *Journal of Materials Science & Technology*, 2015, vol. 31, pp. 946–952.
5. Lass E.A., Stoudt M.R., Williams M.E., Katz M.B., Levine L.E., Phan T.Q., Gnaeupel-Herold T.H., Ng D.S. Formation of the Ni_3Nb δ -phase in stress-relieved Inconel 625 produced via laser powder-bed fusion additive manufacturing. *Metallurgical and Materials Transactions: A*, 2017, vol. 48, pp. 5547–5558. DOI: 10.1007/s11661-017-4304-6.
6. Marchese G., Colera X.G., Calignano F., Lorusso M., Biamino S., Minetola P., Manfredi D. Characterization and comparison of Inconel 625 processed by selective laser melting and laser metal deposition. *Advanced Engineering Materials*, 2016, vol. 19, pp. 1–9. DOI: 10.1002/adem.201600635.
7. Xu F., Lv Y., Xu B., Liu Y., Shu F., He P. Effect of deposition strategy on the microstructure and mechanical properties of Inconel 625 superalloy fabricated by pulsed plasma arc deposition. *Materials & Design*, 2013, vol. 45, pp. 446–455.
8. Grzesik W. Hybrid additive and subtractive manufacturing processes and systems: a review. *Journal of Machine Engineering*, 2018, vol. 18 (4), pp. 5–24. DOI: 10.5604/01.3001.0012.7629.
9. Zverev E., Skeebe V., Martyushev N.V., Skeebe P. Integrated quality ensuring technique of plasma wear resistant coatings. *Key Engineering Materials*, 2017, vol. 736, pp. 132–137. DOI: 10.4028/www.scientific.net/KEM.736.132.
10. Dang J., Zhang H., Ming W. New observations on wear characteristics of solid $\text{Al}_2\text{O}_3/\text{Si}_3\text{N}_4$ ceramic tool in high speed milling of additive manufactured Ti6Al4V. *Ceramics International*, 2020, vol. 46 (5), pp. 5876–5886. DOI: 10.1016/j.ceramint.2019.11.039.
11. Jurić I., Garašić I., Bušić M., Kožuh Z. Influence of shielding gas composition on structure and mechanical properties of wire and arc additive manufactured Inconel 625. *JOM*, 2018, vol. 71, pp. 703–708. DOI: 10.1007/s11837-018-3151-2.
12. Ivancivsky V., Skeebe V., Bataev I., Lobanov D.V. The features of steel surface hardening with high energy heating by high frequency currents and shower cooling. *IOP Conference Series: Materials Science and Engineering*, 2016, vol. 156, p. 012025. DOI: 10.1088/1757-899X/156/1/012025.
13. Keist J.S., Palmer T.A. Development of strength-hardness relationships in additively manufactured titanium alloys. *Materials Science and Engineering: A*, 2017, vol. 693, pp. 214–224. DOI: 10.1016/j.msea.2017.03.102.
14. Balovtsev S.V., Merkulova A.M. Comprehensive assessment of buildings, structures and technical devices reliability of mining enterprises. *Gornyi informatsionno-analiticheskii byulleten' = Mining Informational and Analytical Bulletin*, 2024, no. 3, pp. 170–181. DOI: 10.25018/0236_1493_2024_3_0_170.
15. Montecocchi F., Grossi N., Takagi H., Scippa A., Sasahara H., Campatelli G. Cutting forces analysis in additive manufactured AISI H13 alloy. *Procedia CIRP*, 2016, vol. 46, pp. 476–479. DOI: 10.1016/j.procir.2016.04.034.
16. Shen M.Y., Tian X.J., Liu N., Tang H.B., Cheng X. Microstructure and fracture behavior of TiC particles reinforced Inconel 625 composites prepared by laser additive manufacturing. *Journal of Alloys and Compounds*, 2018, vol. 734, pp. 188–195. DOI: 10.1016/j.jallcom.2017.10.280.
17. Gong Y., Li P. Analysis of tool wear performance and surface quality in post milling of additive manufactured 316L stainless steel. *Journal of Mechanical Science and Technology*, 2019, vol. 33, pp. 2387–2395. DOI: 10.1007/s12206-019-0237-x.
18. Ni Ch., Zhu L., Yang Zh. Comparative investigation of tool wear mechanism and corresponding machined surface characterization in feed-direction ultrasonic vibration assisted milling of Ti–6Al–4V from dynamic view. *Wear*, 2019, vol. 436, p. 203006. DOI: 10.1016/j.wear.2019.203006.

19. Xiong X., Haiou Z., Guilan W. A new method of direct metal prototyping: hybrid plasma deposition and milling. *Rapid Prototyping Journal*, 2008, vol. 14 (1), pp. 53–56. DOI: 10.1108/13552540810841562.
20. Nekrasova T.V., Melnikov A.G. Creation of ceramic nanocomposite material on the basis of ZrO_2 - Y_2O_3 - Al_2O_3 with improved operational properties of the working surface. *Applied Mechanics and Materials*, 2013, vol. 379, pp. 77–81. DOI: 10.4028/www.scientific.net/AMM.379.77.
21. Martyushev N., Petrenko Yu. Effects of crystallization conditions on lead tin bronze properties. *Advanced Materials Research*, 2014, vol. 880, pp. 174–178. DOI: 10.4028/www.scientific.net/AMR.880.174.
22. Zotov V.V., Mnatsakanyan V.U., Bazlin M.M., Lakshinsky V.S., Dyatlova E.V. Povyshenie resursa rabochikh koles tsentrobezhnykh nasosov shakhtnogo vodootliva [Extending the service life of centrifugal dewatering pump impellers in mines]. *Gornaya promyshlennost' = Russian Mining Industry*, 2024, no. 2, pp. 143–146. DOI: 10.30686/1609-9192-2024-2-143-146.
23. Usanova O.Yu., Stolyarov V.V., Ryazantseva A.V. Issledovanie svoystv ionno-implantirovannogo titanovogo splava s pamyat'yu formy, ispol'zuemogo v konstruktsiyakh gornodobyvayushchego oborudovaniya [Investigation of the properties of ion-implanted shape memory titanium alloy used in the construction of mining equipment]. *Ustoichivoe razvitie gornykh territorii = Sustainable Development of Mountain Territories*, 2022, vol. 14, no. 4, pp. 695–701. DOI: 10.21177/1998-4502-2022-14-4-695-701.
24. Cahoon J.R., Broughton W.H., Kutzak A.R. The determination of yield strength from hardness measurements. *Metallurgical Transactions*, 1971, vol. 2 (7), pp. 1979–1983. DOI: 10.1007/bf02913433.
25. Yelemessov K., Baskanbayeva D., Martyushev N.V., Skeebe V.Y., Gozbenko V.E., Karlina A.I. Change in the properties of rail steels during operation and reutilization of rails. *Metals*, 2023, vol. 13, p. 1043. DOI: 10.3390/met13061043.
26. Lou X., Andresen P.L., Rebak R.B. Oxide inclusions in laser additive manufactured stainless steel and their effects on impact toughness and stress corrosion cracking behavior. *Journal of Nuclear Materials.*, 2018, vol. 499, pp. 182–190. DOI: 10.1016/j.jnucmat.2017.11.036.
27. Chen X., Li J., Cheng X., Wang H., Huang Z. Effect of heat treatment on microstructure, mechanical and corrosion properties of austenitic stainless steel 316L using arc additive manufacturing. *Materials Science and Engineering: A*, 2018, vol. 715, pp. 307–314. DOI: 10.1016/j.msea.2017.10.002.
28. Yatsenko V.A., Kryukov Ya.V. Fragmentatsiya i konsolidatsiya proizvodstvennykh tsepochek v mirovoi redkozemel'noi promyshlennosti [Fragmentation and consolidation of production chain in the global rare earth industry]. *Gornaya promyshlennost' = Russian Mining Industry*, 2022, no. 1, pp. 66–74. DOI: 10.30686/1609-9192-2022-1-66-74.
29. Pashkov E.N., Martyushev N.V., Ponomarev A.V. An investigation into autobalancing devices with multireservoir system. *IOP Conference Series: Materials Science and Engineering*, 2014, vol. 66 (1), p. 012014. DOI: 10.1088/1757-899X/66/1/012014.
30. Haidorov A.D., Yunusov F.A. Vakuumnaya termicheskaya obrabotka vysokolegirovannykh korrozionostoikikh stalei [Vacuum heat treatment of high alloy corrosion-resistant steels]. *Nauchno-tekhnicheskie vedomosti SPbGPU = St. Petersburg polytechnic university journal of engineering sciences and technology*, 2017, vol. 23 (1), pp. 226–235. DOI: 10.18721/JEST.230123.
31. Tian Y., McAllister D., Colijn H., Mills M., Farson D.F., Nordin M., Babu S.S. Rationalization of microstructure heterogeneity in INCONEL 718 builds made by the direct laser additive manufacturing process. *Metallurgical and Materials Transactions: A*, 2014, vol. 45, pp. 4470–4483. DOI: 10.1007/s11661-014-2370-6.
32. Krechetov A.A. Obespechenie kachestva svarnykh soedinenii armokarkasa ankernoi krepki putem robotizatsii proizvodstva [Securing the quality of mesh weld joints in bolt support through robotized operation]. *Gornaya promyshlennost' = Russian Mining Industry*, 2021, no. 3, pp. 130–134. DOI: 10.30686/1609-9192-2021-3-130-134.
33. Vidayev I.G., Martyushev N.V., Ivashutenko A.S., Bogdan A.M. The resource efficiency assessment technique for the foundry production. *Advanced Materials Research*, 2014, vol. 880, pp. 141–145. DOI: 10.4028/www.scientific.net/AMR.880.141.

Conflicts of Interest

The authors declare no conflict of interest.